Supporting Information: Tobacco-specific Alkaloids (TSA) Formation in Aged E-cigarette Juices: Mechanistic Insights into Hydroxyl Radical–Initiated Nicotine Oxidation

[1] Xinyang Guo,[†] Bradley H. Isenor,[‡] Kimberly Wong,[†] James Davis,[†] Arthur Chan,[¶] and Ran Zhao*[,†]

[†]*Department of Chemistry, University of Alberta, Edmonton, Alberta T6G 2G2, Canada*

[‡]*Department of Chemistry, University of Toronto, Toronto, Ontario M5S 3H6, Canada*

[¶]*Department of Chemical Engineering and Applied Chemistry, University of Toronto, Toronto, Ontario M5S 1A1, Canada*

E-mail: rz@ualberta.ca

Contents

1 S1. Experimental Layout

This section summarizes the overall design of the experiment (Figure S1).

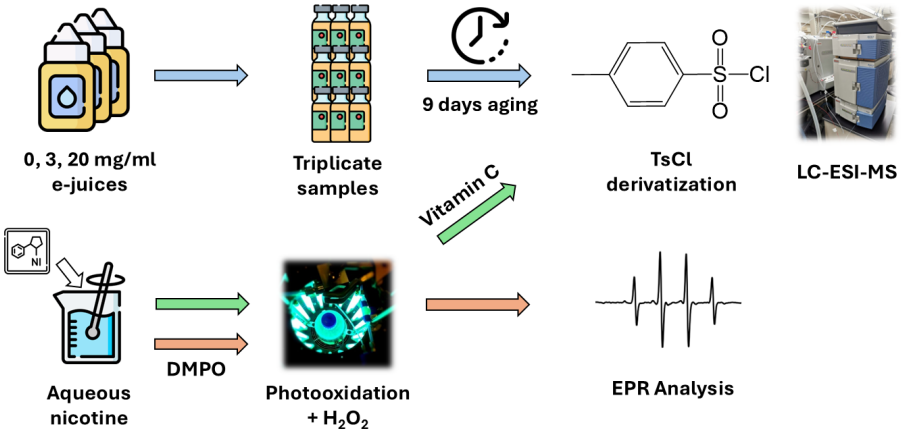

Figure S 1: A brief flowchart of the experimental layout

2 S2. LC-MS settings

This section contains detailed settings of the LC-MS setup (Table S1) and the LC gradient (Table S2).

Table S 1: LC-MS instrument parameters

Table S1. LC-MS instrument parameters	
Injection volume	1 μL
Solvent A	0.1% (v/v) Formic Acid in MQ Water
Solvent B	0.1% Formic Acid in ACN
Gradient	See Table S2
Column	Luna Omega C18 column 150 mm x 2.1 mm x 3 μm
Acquisition Time	16 min
Scanning Mode	Positive
Spray Voltage	4.5 kV
Sheath Gas Flow Rate	40 a.u.
Aux Gas Flow Rate	8 a.u.
Sweep Gas Flow Rate	0 a.u.
Capillary Temp	275℃
Capillary Voltage	35 V
Tube Lens	90 V

Table S 2: Detailed LC gradient

Table S2. Detailed LC gradient			
Time /min	Flowrate μL/min	Solvent A	Solvent B
0	380	99	1
2	380	75	25
12	380	75	25
14	380	1	99
16	380	1	99

3 S3. EPR Sample Preparation and Settings

To prepare the samples for EPR analysis, the samples were injected into capillary tubes (1.8 OD × 1.5 ID × 90 mm) using a micropipette with a gel-loading pipette tip attached (Progene®, 200µL, Round Gel Loaders) so that the solution filled the entire capillary tube and was sealed with Parafilm. The capillary tube was then placed in a clean EPR tube (Wilmad™, Clear Fused Quartz, 4 OD × 3 ID × 250 mm). The prepared sample was immediately measured in a highly sensitive cavity (ER 4119HS). EPR parameters were as follows: a receiver gain of 60 dB with a microwave power of 5.40 mW, an attenuation of 16 dB, a modulation amplitude of 1, a microwave frequency of 9.35 GHz, a sweep width of 200 G, a time constant of 0.01 ms, and a sweep time of 60 s. For each sample, five scans were taken and averaged to obtain the final spectrum. Simulations of EPR spectra and the fitting of simulated spectra were performed using SpinFit in Bruker's Xenon software.

4 S4. Identification of TsCl derivatives

The reaction between amines and TsCl involves a neutral loss of the HCl molecule. The mass-to-charge ratio of protonated TsCl derivatives in ESI-positive mode is determined by the following calculation:

$$[M+H]^+ = M_{molecule} + M_{TsCl} - M_{HCl} + 1 \tag{1}$$

As mentioned in the main text, by assuming that the only source of sulfur in the sample is TsCl, the signature isotopic peak profile at $[M+2]^+$ of sulfur-containing species can be used to confirm TsCl derivatives. This peak profile is due to the mass difference between ^{34}S and ^{14}C, where the mass of M(^{34}S) is smaller than M(^{14}C) or M($^{13}C_2$). Consequently, the peak at the $[M+2]^+$ position will split, with the lighter peak referring to M(^{34}S). In addition, M(^{34}S) would have a higher intensity due to the natural abundance of ^{34}S (4%) being higher than ^{14}C (1%). In Figure S2, we illustrated this identification procedure by showing a TsCl-derived nornicotine (Ts-nornicotine) under high-resolution MS (resolution = 50000).

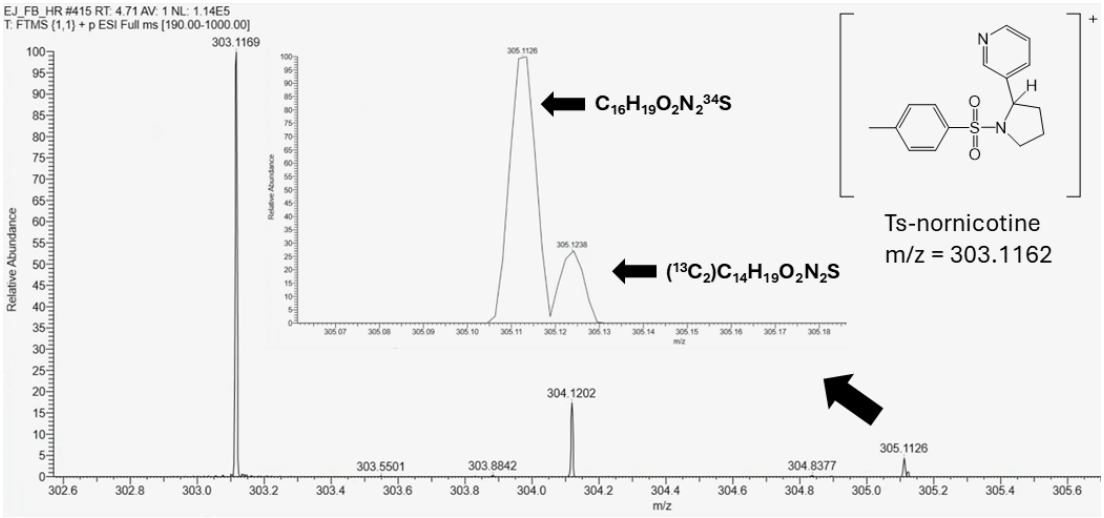

Figure S 2: High-resolution mass spectrum of nornicotine

5 S5. Supporting EPR Results

5.1 S5.1. EPR Spectra for Quality Control

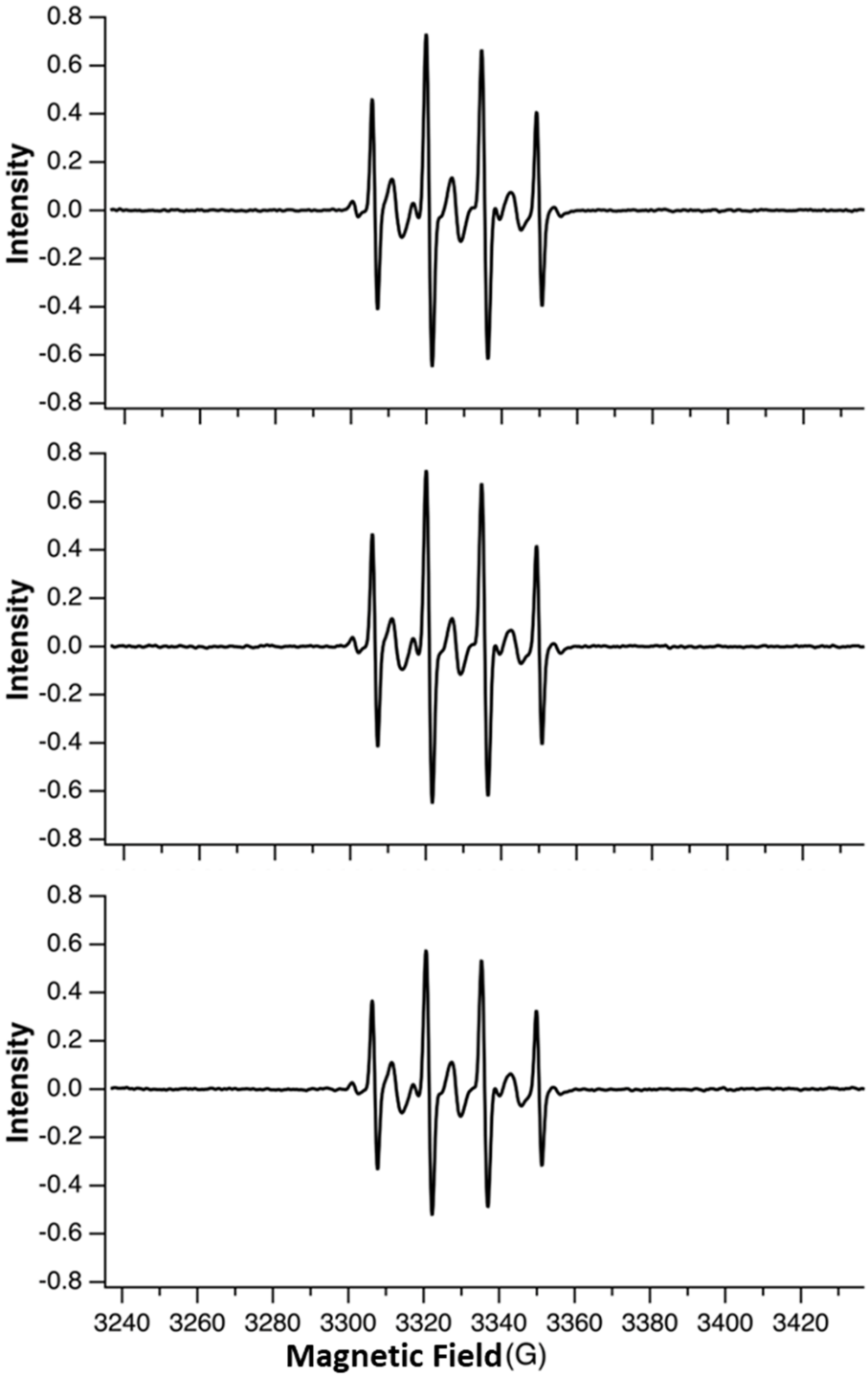

Figure S 3: Triplicate EPR spectra of 100 mM DMPO + 1.25 M nicotine + 1.25 M H_2O_2 after 5 minutes of UV irradiation.

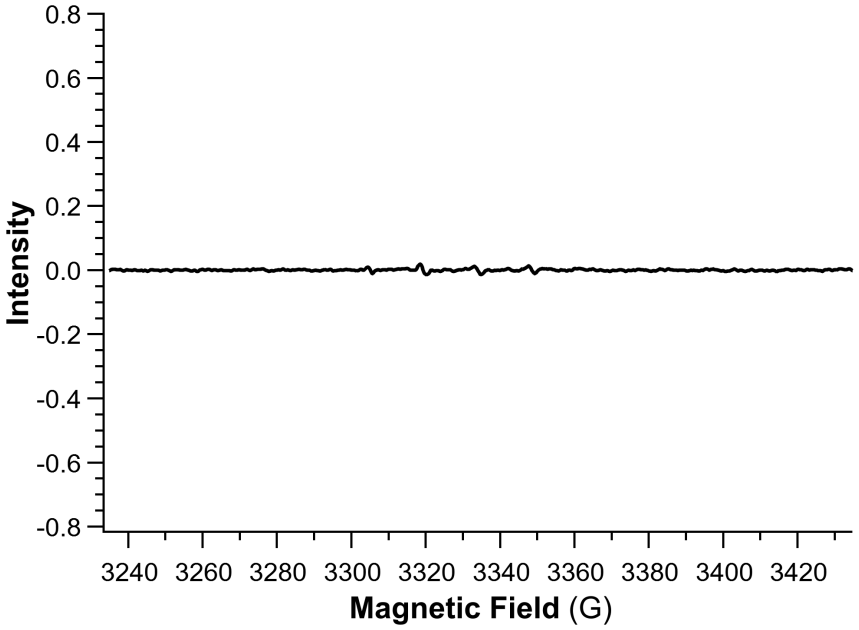

Figure S 4: EPR spectra of 100 mM DMPO + 1.25 M H_2O_2 + 1.25 M nicotine without UV irradiation.

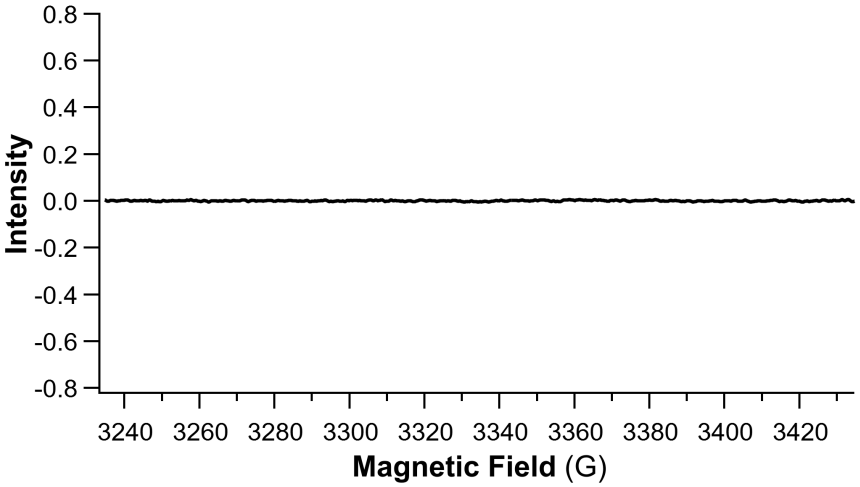

Figure S 5: EPR spectra of 1.25 M nicotine after 5 minutes of UV irradiation.

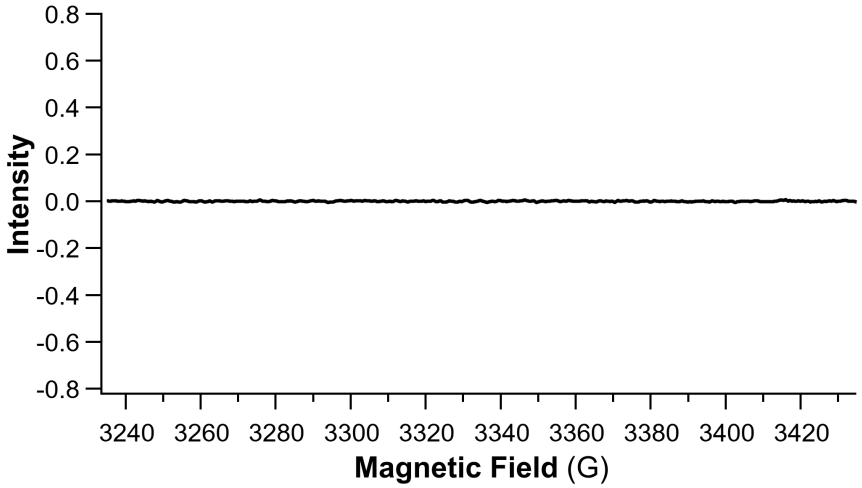

Figure S 6: EPR spectra of 1.25 M H_2O_2 + 1.25 M nicotine, without DMPO, after 5 minutes of UV irradiation.

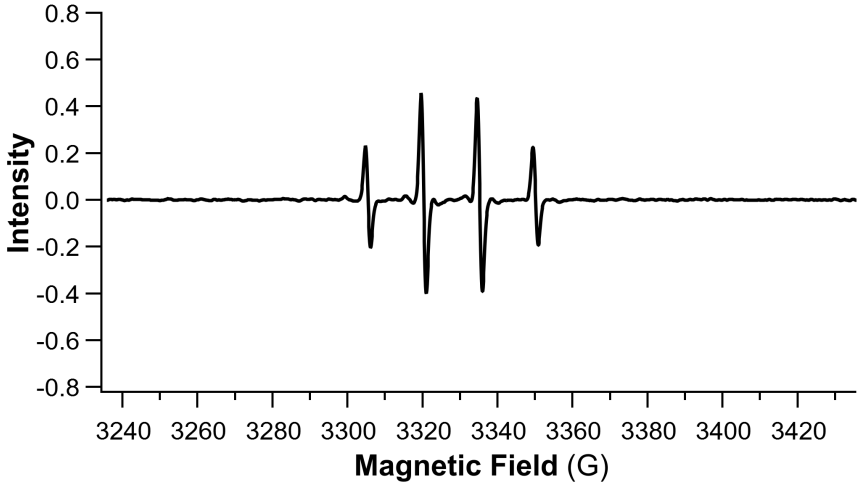

Figure S 7: EPR spectra of 100 mM DMPO + 1.25 M H_2O_2, without nicotine after 5 minutes of UV irradiation.

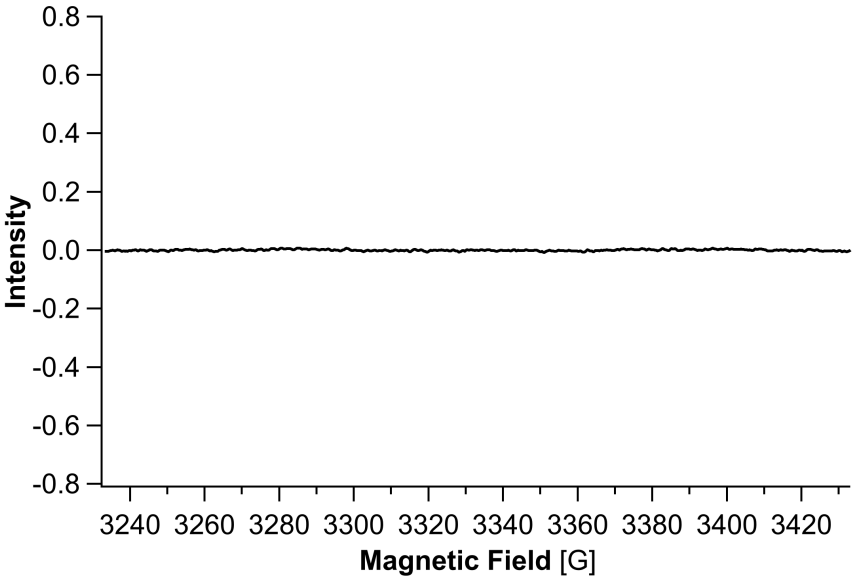

Figure S 8: EPR spectra of aged 20 mg/mL EJ, without the addition of H_2O_2 or UV irradiation.

5.2 S5.2. Simulated EPR Spectra

We simulated a series of EPR spectra (Figure S9 to S12) to determine the potential identity of the radicals generated during the photooxidation of nicotine.

A previous study had proposed that methyl radicals ($\cdot CH_3$) forming CH_3 adducts (DMPO-CH_3) are responsible for a triplet pattern,[1] but the hyperfine splitting behavior of the CH_3 adduct should provide a 6-peak splitting pattern of 1:1:1:1:1:1, which is inconsistent with the observed peak pattern. Furthermore, we were unable to fit a simulated DMPO-CH_3 spectrum to our measured spectrum (Figure S9). Similarly, we also examined the possibility of a DMPO-H adduct, and its spectrum produces peaks in a 1:1:2:1:2:1:2:1:1 splitting pattern, where smaller peaks would be masked by DMPO-OH. However, when the DMPO-H spectrum was fitted to the measured spectrum, the spectrum we observed from the EPR was missing 2 key peaks of DMPO-H in the lower and higher fields (located at 3289 and 3366 G), ruling it out as a match (Figure S10).

Another possibility for DMPO being a triplet is if the structure of DMPO is altered so that there is no H atom close to the O-centered radical of the DMPO radical species to

influence the hyperfine splitting. We hypothesize that the observed triplet is a result of DMPO undergoing a transformation to a nitroxide radical, which explains the 1:1:1 splitting pattern we observed. The transformation of DMPO to a nitroxide radical has been observed previously in the presence of a trioxolane,[2] which is unlikely in our reaction. For the nitroxide, we measured a hyperfine splitting constant of A_N = 15.9 G (water used as the solvent), consistent with the literature value of 15.5 G (CH_2Cl_2 used as the solvent).[2] We expect some difference in our hyperfine splitting constant, given the effect solvents can have on hyperfine splitting.[3]

The fitting of the simulated spectra of only DMPO-OH and the nitroxide did not account for all the observed peaks, most notably the small peaks in the lower and higher fields, bracketing DMPO-OH and the nitroxide (Figure S11). However, by simulating a spectrum for an unknown DMPO adduct (DMPO-Y) with a nuclear spin of I = 0 on the atom of the adduct bonded to DMPO, with hyperfine splitting constants of A_N = 15.8 and A^H = 21.6, we were able to obtain a simulated spectrum that matched the observed spectrum (Figure S12). Consequently, our observed spectrum is the combination of nitroxide and DMPO-Y radicals.

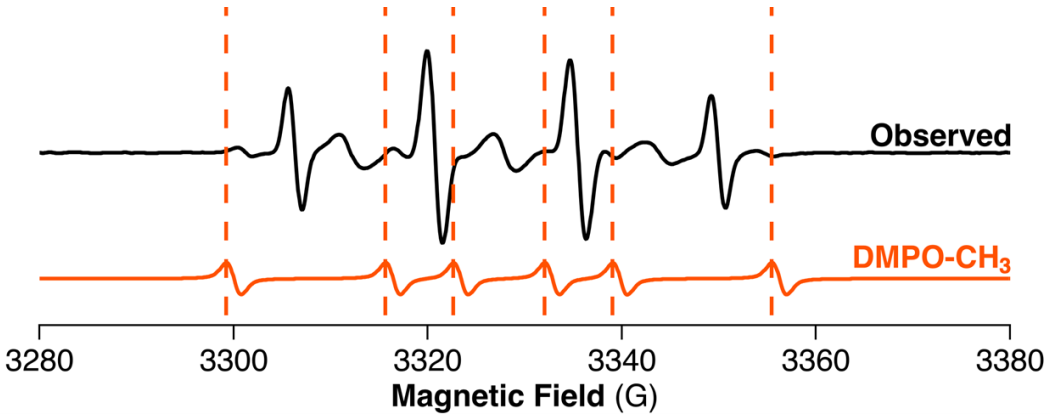

Figure S 9: The observed EPR spectrum (black) of sample [a] (1.25 M H_2O_2, 1.25 M nicotine, 100 mM DMPO) and simulated spectrum of DMPO-CH_3 (orange). Dashed lines visualize the positions of peaks for DMPO-CH_3.

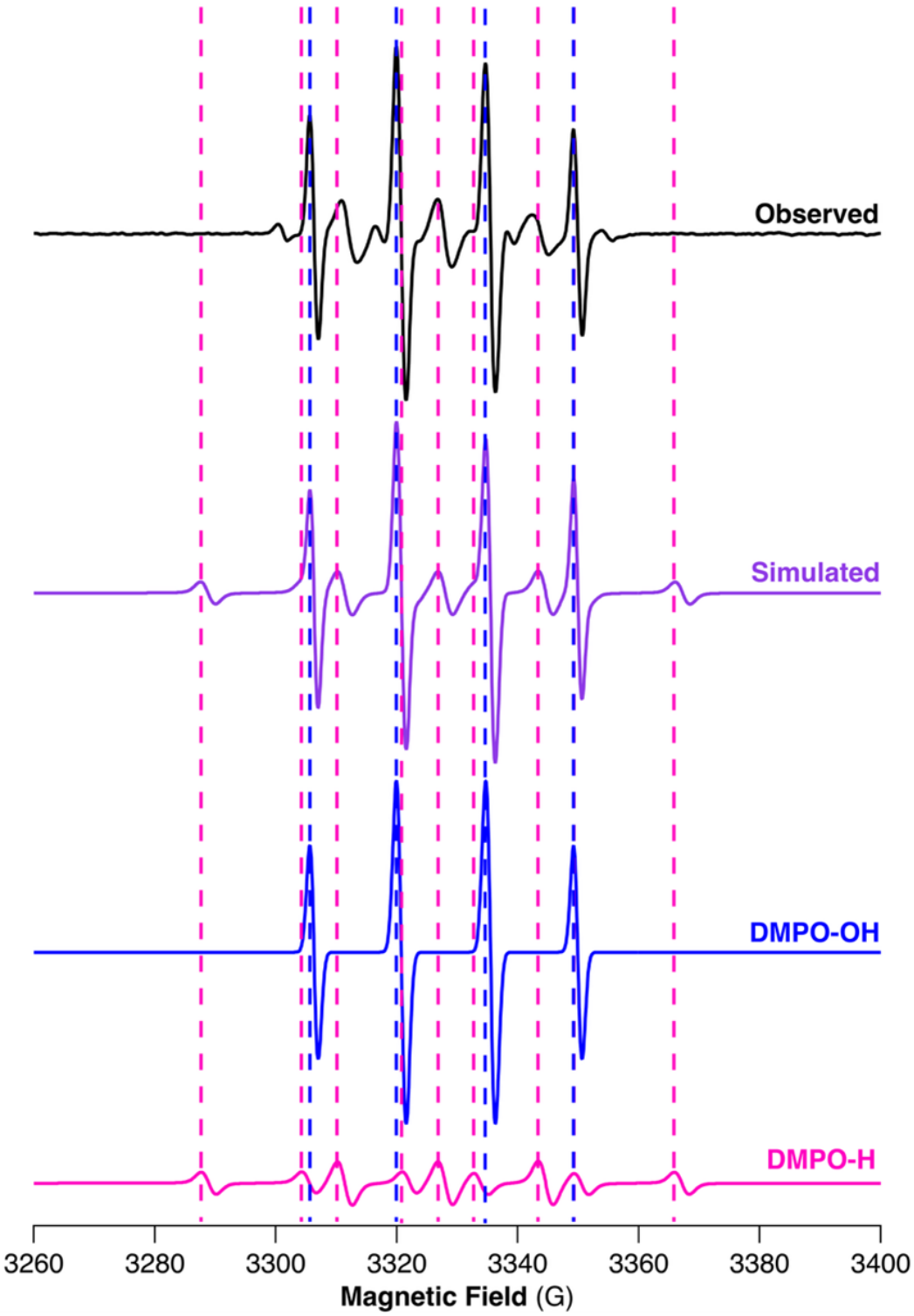

Figure S 10: The observed EPR spectrum (black) of sample [a] (1.25 M H_2O_2, 1.25 M nicotine, 100 mM DMPO) and simulated spectrum of DMPO-OH and DMPO-H (purple). Separate simulated spectra of DMPO-OH (blue) and DMPO-H (pink) with dashed lines visualizing the positions of the peaks for the different radicals trapped by DMPO.

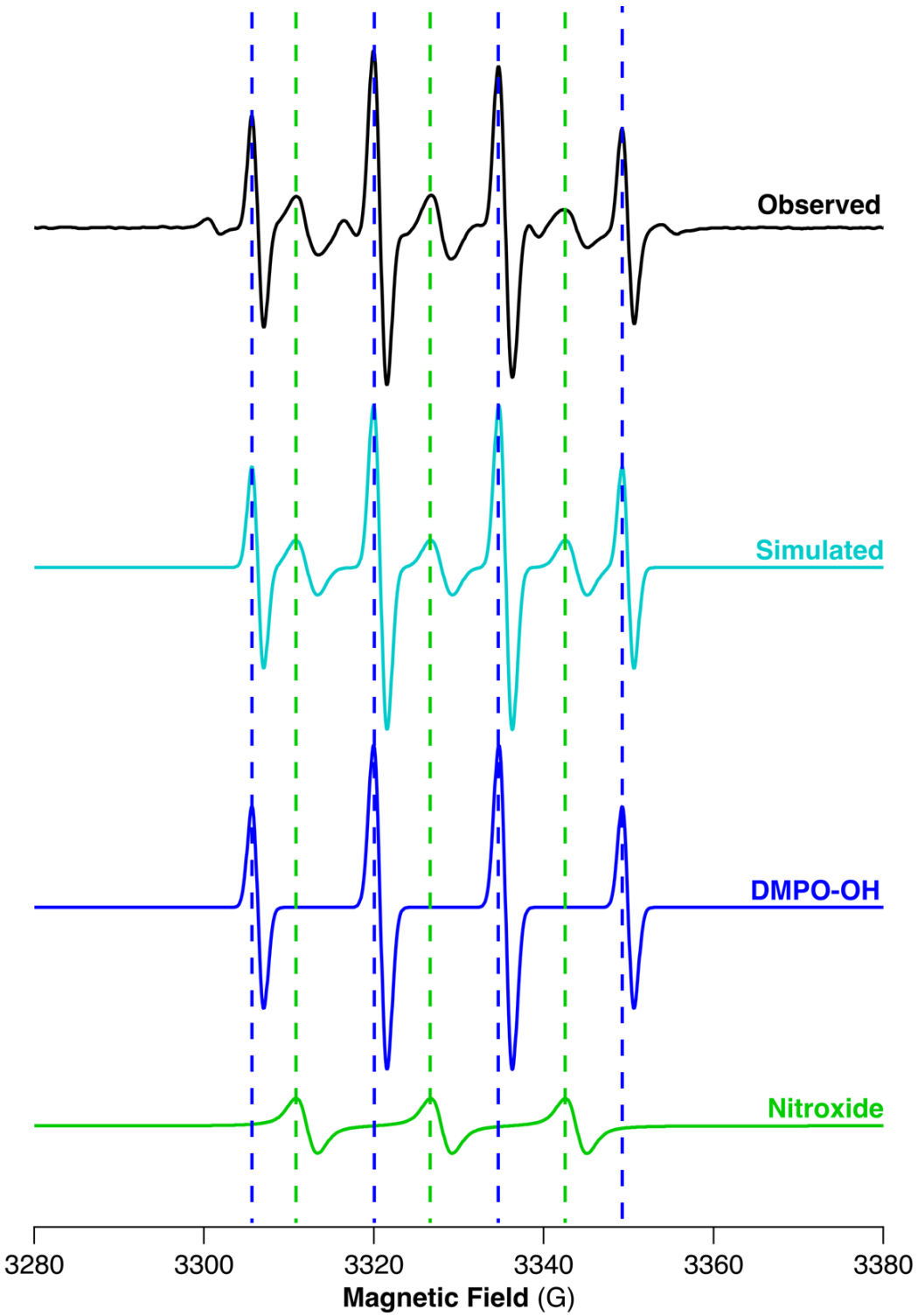

Figure S 11: The observed EPR spectrum (black) of sample [a] (1.25 M H_2O_2, 1.25 M nicotine, 100 mM DMPO) and simulated spectrum of DMPO-OH and nitroxide radical (teal). Separate simulated spectra of DMPO-OH (blue) and nitroxide radical (green) with dashed lines visualizing the positions of the peaks for the different radicals trapped by DMPO.

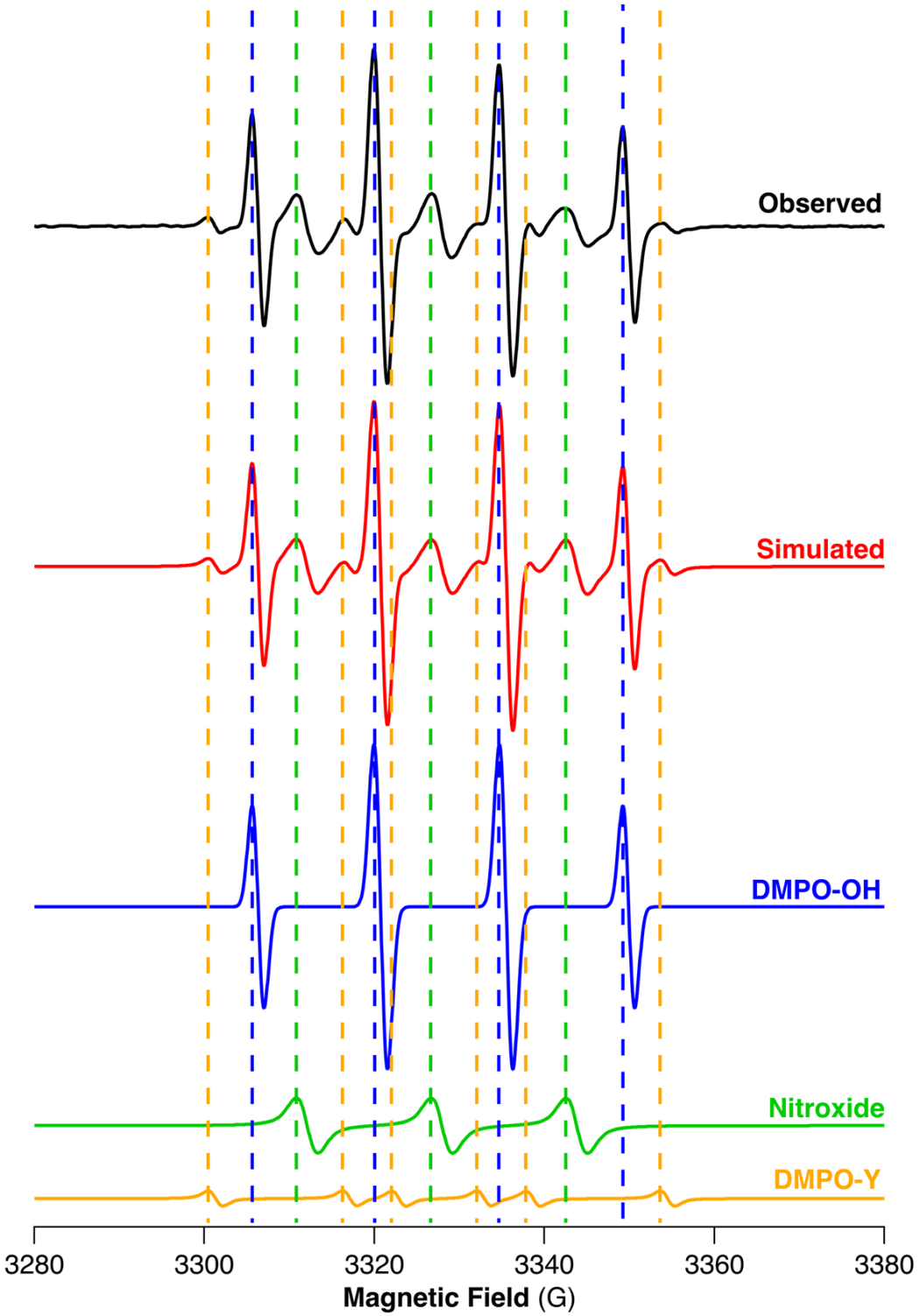

Figure S 12: The observed EPR spectrum (black) of sample [a] (1.25 M H_2O_2, 1.25 M nicotine, 100 mM DMPO) and simulated spectrum of DMPO-Y and nitroxide radical (red). Separate simulated spectra of DMPO-OH (blue), nitroxide radical (green), and DMPO-Y (yellow) with dashed lines visualizing the positions of the peaks for the different radicals trapped by DMPO.

References

(1) Chauvin, J.; Judée, F.; Yousfi, M.; Vicendo, P.; Merbahi, N. Analysis of reactive oxygen and nitrogen species generated in three liquid media by low temperature helium plasma jet. Scientific Reports **2017**, 7.

(2) Pryor, W. A.; Govindan, C. K. Oxygen-atom-transfer reactions from a carbonyl oxide (produced from a 1, 2, 3-trioxolane) to electron-deficient unsaturated compounds. Journal of the American Chemical Society **1981**, 103, 7681–7682.

(3) Buettner, G. R. Spin Trapping: ESR parameters of spin adducts 1474 1528V. Free Radical Biology and Medicine **1987**, 3, 259–303.